LUNAR IMPACT MELTS AND OTHER THINGS THAT FLOW ON THE MOON. J. B. Plescia
Applied Physics Lab, Johns Hopkins University, Laurel, MD

Introduction: Impact melt is observed over a range of impact sizes on the Moon, extending from basins (e.g., Imbrium, SPA) to craters as small as ~100 m. Impact melt occurs as the floor filling of basins and large complex craters, as ponds and flows within the down-dropped blocks around the terraced margins, as isolated ponds, and as flows and narrow dark stringers extending from the rim (Fig. 1a). In addition to features that are easily interpreted as impact melt flows, a second class of flow features is observed associated with ejecta at craters such as Giordano Bruno (Fig. 1c).

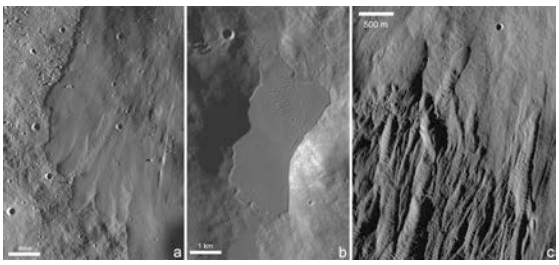

Fig. 1. Impact melt flows at Korolev X (a) and Tycho (b). Flow material with distal ejecta at Giordano Bruno (c).

Understanding the volume of impact melt retained on the crater floor and rim, the rheologic properties of the melt, and the origin of other flow features is critical in understanding the details of the impact catering process in terms of energy partition, excavation, ejecta emplacement and the nature of lunar samples.

Because impact-melt is a molten silicate rock, its rheology can be understood in the same context as that of lava flows and the analyses and modeling of terrestrial and planetary lava flows [1-10] can be used as a basis to study planetary impact melt flows.

Melt Pool Volume: Studies of the volume of impact melt found on the floor of simple lunar craters [11] show that the melt volume is typically less than predicted than would be expected based on modeling studies [12-13]. Similar discrepancies are observed on the mare and in the highlands. The cause of this difference is unclear and may result from imprecision in the models, imprecision of the volume estimations, or a wider influence of specific impact conditions than are reflected in the models.

Melt Flow Rheology: LROC NAC images, LROC NAC DTMs, WAC DTMs, and LOLA profile data can be used to define the morphometry of impact melt flows including: flow width, channel and levee width, thickness, surface fold wavelength and amplitude, and topographic slope. Flow length is unconstrained beyond establishing a minimum length. The upstream end of a melt flow is typically truncated by the crater rim; in other cases, it is buried by subsequent flows.

Rheologic models to calculate yield strength employ different morphometric parameters as well as local gravity and flow density. In some cases (e.g., Fig 1b) the surface of the flow is folded and the fold wavelength and amplitude can be used to constrain the rheology [14-15]. Estimates of viscosity and effusion rate are derived from the yield strength and other physical constants. A flow will have a width and thickness controlled by rheology only if the flow is topographically unconstrained. Similarly, it is assumed that the substrate is smooth such that the flow is not impeded by large-scale roughness. In some cases these assumptions are valid; in other cases they are not.

Flows of impact melt extending downslope from the rim and dark stringers extending across the ejecta are observed only at the freshest craters. The stringers rapidly disappear, followed by the flows as a regolith develops. Pools of melt on the floor and rim terraces persist much longer.

Impact melt is initially deposited on the rim and begins to flow downslope. It can continue downslope as a broad sheet or coalesce into a well-defined flow. Multiple pulses of melt deposition are indicated by numerous overlapping lobes. Individual lobes have sufficient momentum to ride up and over topographic obstacles and to bulldoze boulders. Cooling of the flow occurs by radiation; conduction of heat into the subsurface is negligible because of the low thermal conductivity of the regolith. Ingestion of boulders and other debris during deposition and flow can significant influence the cooling as such material would be cold.

Flow material associated with about fifty craters, with visually well-defined impact melt flows extending down slope, have been examined. For those whose morphometric parameters could be collected, multiple profiles along individual flows were measured and yield strengths estimated. Table 1 lists example results.

Lobate Flows: Lobes of material (Fig. 1c) are associated with the distal continuous ejecta at Giordano Bruno and other craters. This material exhibits morphological characteristics typically observed for lava and impact melt flows including lobate margins, channels, levees and surface folding (Fig. 2). The flows often begin in a theater-headed depression and extend downslope; in other cases the source area of the flow is hidden beneath ejecta. In case where channel-forms are absent, the surface has a convex shape.

Table 1. Modeled Yield Strengths			
Crater	**Lat. / Long.**	**D (km)**	**τ (Pa)**
Lichtenberg B	33.3° / 298.5°	5.2	4×10^1
Giordano Bruno	35.9 / 102.8	22	10^2
Fersman South	13.6° / 234.5°	9	10^3
Byrgius	-24.6° / 296.2°	19	$1\text{-}2 \times 10^3$
Mandel'shtam F	5.1° / 266.1°	15	9×10^3
Das G	-29.0° / 227.2°	11.7	3×10^4
O Day M	-31.6° / 157.0°	12.3	4×10^4
Tycho North	-41.18° / 348.6°	86	4×10^4
Gibbs*	-18.4° / 84.3°	4.8	$1\text{-}9 \times 10^3$
Pierazzo*	-3.3°/ 100.2°	8.5	$10^3\text{-}10^4$
* flow of uncertain origin			

The orientation of such flows can be parallel to the depositional direction of the continuous ejecta (not necessarily downslope) or down the maximum topographic slope. In some cases (Fig. 2), the flow is observed to turn from the direction of the continuous ejecta to the local topographic slope. The orientations of the flows suggest they were emplaced along with the continuous ejecta and had sufficient momentum avoid the influence of the local slope. Once the flow slows, it turned downslope before coming to a halt.

The origin of this material is unclear. Bray et al. [16] suggest that it is impact melt contained within the clastic ejecta that leaks out when the clastic ejecta flow stalls. In this model the melt drains from the ejecta to form a melt flow extending downslope. Alternatively, they may be more akin to a landslide and consist of remobilized clastic ejecta.

Discussion: Impact melt flows exhibit a range of morphologies and a range of rheologic properties. Yield strengths range over three orders of magnitude from 10^1 to 10^4 Pa between individual craters and among flows at a given crater. The modeled yield strengths overlap those associated with basaltic lavas at Kilauea and Mauna Loa [17-18]. The melt values are also consistent with previous estimates of impact melt rheology [1, 17, 19].

Modeled yield strengths do not correlate with crater diameter (i.e., energy of the impact event) or with target type (mars vs. highlands). Yield strengths do correlate with flow morphology. The low yield strength values are consistent with the thin coatings (unresolved thickness) of melt locally found the surface and on large boulders. The high values are consistent with large, bulbous morphology of some flows (e.g., the north flank of Tycho).

Applying the rheologic models used for the melt flows to the lobate flows indicates yield strengths similar to the melt flows (Table 1). The small-scale morphology of these features suggests that they are landslide deposits rather than impact melt flows.

Conclusions: Lunar impact melt flows have rheologies similar to that of terrestrial basalts, however yield strengths range over three orders of magnitude. The variations likely reflect small-scale spatial variations in the melting of target rocks and the initial temperature of the melt. The lobate flow features observed with the ejecta have similar rheology, but are interpreted as landslides rather than melt flows.

References: [1] Hulme G. (1974) *J. Royal Ast. Soc.*, *39*, 361-383 [2] Hulme G. & Fielder G. (1977) *Phil. Trans. Royal Soc. London A*, 285, 227-234. [3] Baloga S. (1987) *JGR*, *92*, 9271-9279 [4] Baloga S. & Pieri D. (1986) *JGR*, *91*, 9543-9552 [5] Crisp J. & Baloga S. (1994) *JGR*, *99*, 11,819-11,831 [6] Glaze L. & Baloga S. (2006) *JGR*, *111*, E09006, doi:10.1029 / 2005JE002585 [7] Glaze L. et al. (2009) *JGR*, *114*, E07001, doi:10.1029 / 2008JE003278 [9] Keszthelyi L. (2012) *LPSC 43rd*, Abstract 2567 [10] Wilson L. & Head J. (2003) *JGR*, *108*, doi:10.1029 / 2002JE001909 [11] Plescia, J. et al. (2014) LPSC 45th, Abstract 2141 [12] Cintala M. & Grieve R. (1998) *Met. Plant. Sci.*, *33*, 889-912 [13] Grieve R. and Cintala, M. (1992) *Meteoritics*, *27*, 526-538 [14] Fink, J. & Fletcher, R. (1978) *JVGR, 4,* 151-170 [15] Gregg, T. et al. 1998, JVGR 80, 281-292 [16] Bray, V. et al. (2013) *LPSC 44th*, Abstract 2782 [17] Moore H. & Schaber G. (1975) *LPSC 6th*, 101-118 [18] Moore, H. (1987) *USGS Prof. Paper 1350*, Chapter 58 [19] Denevi B et al. (2012) *Icarus*, *219*, 665–675.

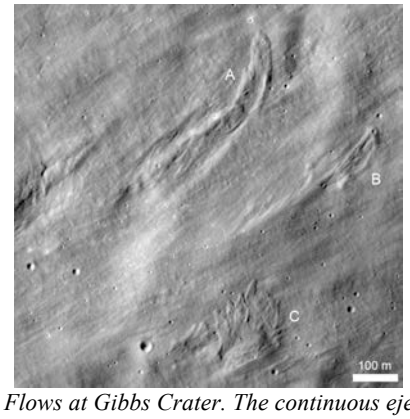

Fig 2. Flows at Gibbs Crater. The continuous ejecta is deposited to the NE across the slope (9° along the striations). Flow follows then turns northward down the steeper topographic slope (15°). M103954588R.